Improved crystalline structure and H_2S sensing performance of CuO-Au-SnO_2 thin film using SiO_2 additive concentration

Shang-Wei Tsai [1], **Jin-Chern Chiou** [1, 2, *]

[1] Department of Electrical Engineering, National Chiao-Tung University, Hsinchu, Taiwan 30010 (R.O.C.)

[2] School of Medicine, China Medical University, Taichung, Taiwan 40402 (R.O.C.)

[*]**Corresponding author:**

Tel: 886-3-5731881

Fax: 886-3-5715998

E-mail address: chiou@mail.nctu.edu.tw

Present address: Room 746 Technology 5th Building, 1001 University Road, Hsinchu, Taiwan 30010 (R.O.C.)

Abstract

In situ SiO_2-doped SnO_2 thin films were successfully prepared by liquid phase deposition. The influence of SiO_2 additive as an inhibitor on the surface morphology and the grain size for the thin film has been investigated. These results show that the morphology of SnO_2 film changes significantly by increasing the concentration of H_2SiF_6 solution which decreases the grain size of SnO_2. The stoichiometric analysis of Si content in the SnO_2 film prepared from various Si/Sn molar ratios has also been estimated. For the sensing performance of H_2S gas, the SiO_2-doped Cu-Au-SnO_2 sensor presents better sensitivity to H_2S gas compared with Cu-Au-SnO_2 sensor due to the fact that the distribution of SiO_2 particles in grain boundaries of nano-crystallines SnO_2 inhibited the grain growth (< 6 nm) and formed a porous film. By increasing the Si/Sn molar ratio, the SiO_2-doped Cu-Au-SnO_2 gas sensors (Si/Sn = 0.5) exhibit a good sensitivity (S = 67), a short response time ($t_{90\%}$ < 3 s) and a good gas concentration characteristic (α = 0.6074). Consequently, the improvement of the nano-crystalline structures and high sensitivity for sensing films can be achieved by introducing SiO_2 additive into the SnO_2 film prepared by LPD method.

Keywords: Tin oxide, Liquid phase deposition, SiO_2 additive, H_2S sensor

1. Introduction

SnO_2 is a semiconductor with a wide band-gap (Eg = 3.6 eV) that has been used in many important applications, including photoelectric devices [1], solar cells [2] and gas sensors [3–5]. The latter particularly benefit from SnO_2 thin film because of its structure, electrical properties and ability to detect various reducing gases, such as CO [6], ethanol [7] and H_2S [8-10]. Among of them, the hydrogen sulfide (H_2S) is a toxic gas produced from oil and natural gas, food processing and bacterial breakdown of organic matter or wastes produced by human and animal. The detection and monitoring of H_2S gas is important in the areas of oil and natural gas exploration, amenity of living environments and diagnosis in dentistry.

The sensing properties of SnO_2 sensors to H_2S gas have been shown to be influenced by many factors such as metal oxide additives, grain size and microstructure [11, 12]. In the metal oxide additives, most research and development of SnO2-besed H2S gas sensors are focused on Cu or Ag [5, 8-11], which utilize the heterocontacts between p-type CuO or Ag_2O and n-type SnO2 to form p-n junction and chemical affinity of CuO or Ag_2O to H_2S. When the additive-doped SnO_2 sensor exposes in H2S gas, the p-n junction is disrupted and the resistance of sensor drops down dramatically.

On the other hand, the SnO_2 sensing films tend increasingly to have nano-crystalline structures that usually are porous and have a relatively high specific surface area. The several interfaces between the nano-grains that interact with gas molecules effectively improve the diffusion properties while greatly increasing the sensitivity of the sensing film to gas. Accordingly, the effect of additives as inhibitors on the SnO_2 film have been studied by using various methods, such as sintered pastes [12], sol-gel [13, 14] and hydrothermal [15, 16].

In this study, the liquid phase deposition (LPD) was firstly used to deposit the SnO_2 film as gas sensing material, which nano-crystalline structures were improved by adding impurities in the treatment solution. Up to now, the LPD method has been widely applied to deposit many transition metal oxide films [17-19]; the preparation of which is based on the ligand-exchange hydrolysis of a metal-fluoro complex and an F^- consumption reaction with boric acid or aluminum metal.

The purpose of this study is to discuss the effect of SiO_2 as an inhibitor on the grain growth of SnO_2 film. In this paper, we report a SiO_2-doped Cu-Au-SnO_2 H_2S sensor. The sensing material is made of introducing various

concentration of SiO_2 into the SnO_2 film during the liquid phase deposition. The proper amounts of Cu and Au as catalysts were coated on the SiO_2-doped SnO_2 surface by dip-coating method. The nanostructure of SiO_2-doped SnO_2 was characterized with X-ray diffraction (XRD), scanning electron microscopy (SEM), and atomic force microscopy (AFM). The stoichiometric analysis of Si content in the SnO_2 film prepared from various Si/Sn molar ratios has been estimated. The response properties of fabricated sensors to staircase concentration of H_2S and the recovery time in air have also been investigated and discussed.

2. Experimental

2.1 Deposition of SiO_2-doped SnO_2 film

LPD-SnO_2 thin films were prepared following the method given in Ref. [13]. Two substrates, oxidized silicon wafer and alumina, were used in this study. The starting reagent was SnF_2. The initial solution was prepared by dissolving SnF_2 powder in deionized (DI) water at room temperature with stirring, as the concentration was maintained at 0.1 M. The substrates were immersed vertically in the solution for ten hours at 60 °C with stirring to deposit the SnO_2 film.

SiO_2-doped SnO_2 films were prepared from growth solution at various Sn/Si molar ratios. First, excess silicic acid powder ($SiO_2 \cdot xH_2O$) was added to a commercial (RDH, Germany) 34 wt% hydrofluorosilicic acid (H_2SiF_6, 3.09 M) solution and thoroughly mixed by stirring for six hours to saturate at room temperature. After saturation, the undissolved silicic acid powders were filtered out using a 0.2 μm Teflon filter. Then, the filtered 3.09 M saturated H_2SiF_6 solution was poured into the above 0.1 M SnF_2 solution. Growth solutions that contained three molar ratios of Si/Sn, 0.25, 0.33, and 0.5, were prepared. Before the substrates were immersed for deposition, various quantities of 0.5 M boric acid (H_3BO_3) were added with stirring and the molar ratio of boric acid to H_2SiF_6 in the growth solution was maintained at 2:1.

After ten hours of deposition, the substrate was removed, washed with DI water, and then dried at 70 °C. The calcination of films was carried out at the temperature varied from 300 to 700 °C with an increase of 100 °C for 1 hour in air.

The crystalline phase of the films was identified from grazing incident angle X-ray diffraction (Bede, D1) spectra obtained using Cu Ka radiation. The

surface roughness and morphology of the films were determined by scanning electron microscopy (Hitachi, S-4700I) and atomic force microscopy (Digital instrument, Dimension 3100). The chemical compositions of films were analyzed by high resolution X-ray photoelectron spectrometry (ULVAC-PHI, PHI Quantera SXM).

2.2 Fabrication of gas sensors and measurement of gas response characteristics

An alumina substrate with Au electrodes on both sides and RuO_2 on backside as a heater was prepared by screen-printing. The sensing area of the tin oxide was defined using a patterned photoresistor on the front of substrate whose backside was coated with the photoresistor as a passivation layer. Following deposition, the whole surface was covered with tin oxide. Then, the photoresistor was removed using acetone and a patterned SnO_2 was obtained by lift-off. After calcination of SnO_2 film at 600 °C for 1 hour in air, this polycrystallized films were immersed firstly in 2.5 mM cupric nitrate trihydrate ($CuNO_3 \cdot 3H_2O$) solution for 20 seconds, pulled up slowly, and then dried at 60 °C in air, followed by calcination at 600 °C for 30 minutes in air. The doping process of Au catalyst was carried out similarly above in 30 mM hydrogen tetrachloraurate trihydrate ($HAuCl_4 \cdot 3H_2O$), but the calcining temperature is at 350 °C. The calcination temperatures of catalysts were based on the results of thermal gravimetric analysis of the catalyst as shown in Fig. 1.

The sensor chips were wire bonded and suspended in air using Pt-wires. To determine the gas-sensing properties, the sensors were placed in a close chamber at room temperature and heated them up to a temperature between 250 and 300 °C. When H_2S was introduced into the chamber by using an injector and disturbed with a fan, the film resistance decreased. The response of each sensor to H_2S at constant concentration and the recovery time in air were measured by continuously recording the resistance of the sensor. In this study, the gas sensitivity was defined by $S = (R_a - R_g)/R_a$, where R_a and R_g are the electric resistances between Au electrodes before and after introduction of H_2S, respectively.

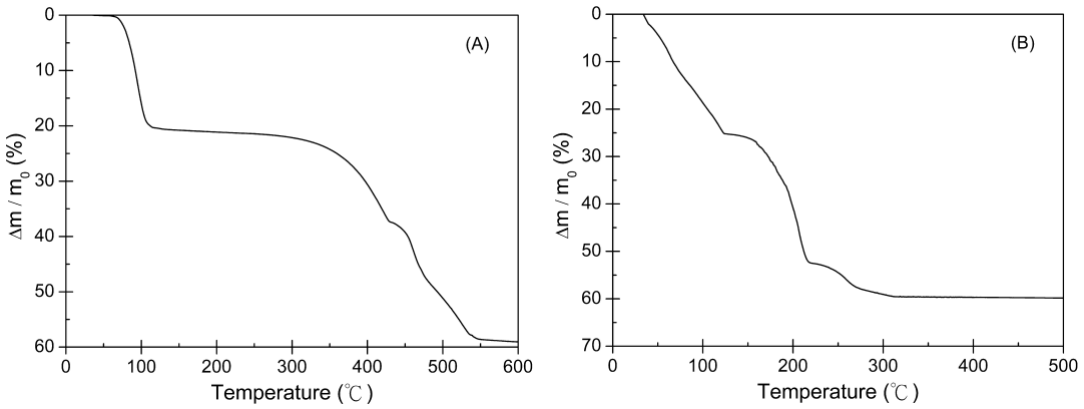

Fig. 1. The thermal gravimetric analysis curves: (A) $Cu(NO_3)_2 \cdot 3H_2O$, (B) $HAuCl_4 \cdot 3H_2O$.

3. Results and discussion

3.1 Microstructure of thin films

Figure 2(a) shows the grazing incident angle X-ray diffraction (GIAXRD) patterns of SnO_2 films that were calcined at various temperatures for 1 hour in air. The diffraction peak from the (110) crystal face was the largest, and the ratio between its intensity and those of the reflex intensities of the (101) and (211) faces agrees with the pattern of the tetragonal stannic oxide crystal [20]. The patterns indicate that the thin films belong to the rutile phase of SnO_2. Figure 2(b) shows the effect of adding H_2SiF_6 on the diffraction peaks of the SnO_2 film. The half-width of the diffraction peaks in SiO_2-doped SnO_2 films increases with the Si/Sn molar ratio. At Si/Sn molar ratio of 0.5, effective grain growth inhibiting was clearly observed by much less peak sharpening as compared to the pure SnO_2 film and all the diffraction peaks also match with rutile phase. This result indicates that the SiO_2-doped SnO_2 film contains smaller grains than a pure SnO_2 film. Figure 3 plots the grain sizes of pure SnO_2 and SiO_2-doped SnO_2 films prepared at various Si/Sn molar ratios as functions of calcination temperature. Here, the grain size is estimated using the following equation, Eq. (1), from the half-width of the (110) diffraction peak based on the assumption that peak broadening occurs mainly because of the size effect [21].

$$D_{110} = 0.9l / b_{1/2} \cos q \qquad (1)$$

where D_{110} denotes the grain size, l = 1.541 Å, $b_{1/2}$ is the half-width of the (110)

diffraction peak, and q is the diffraction angle. The grains grow with the calcination temperature, but become more torpidly as the Si/Sn molar ratio increases. This result proves that doping with SiO_2 can effectively inhibit the grain growth of SnO_2.

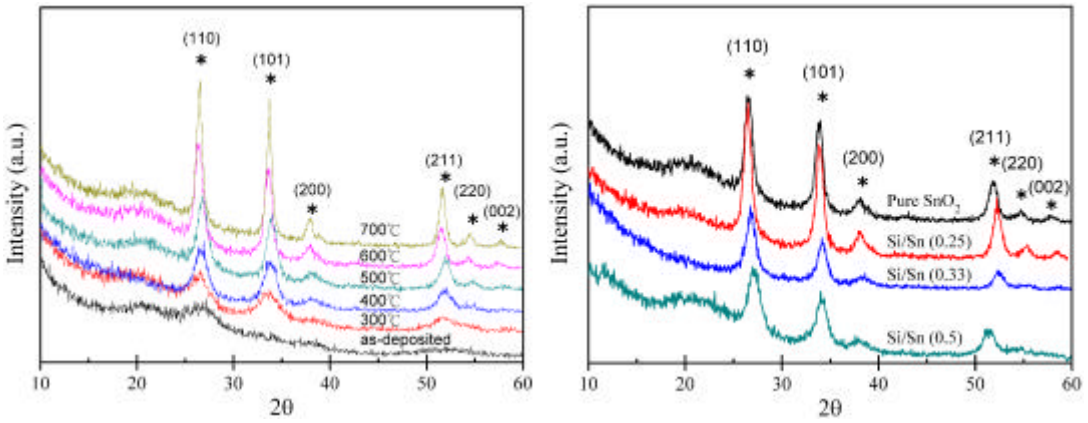

(a) (b)

Fig. 2. X-Ray diffraction patterns of SnO_2 films: (a) pure SnO_2 films calcined at various temperatures, (b) pure SnO_2 and SiO_2-doped SnO_2 thin films calcined at 600 ˚C for 1 hour in air as a function of the molar ratio of Si/Sn.

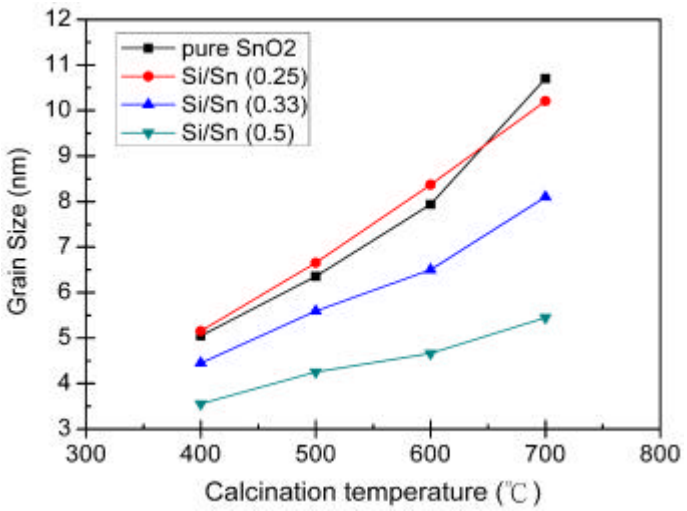

Fig. 3. The grain sizes of SnO_2 films prepared at various Si/Sn molar ratios as a function of calcination temperature.

Figure 4 shows SEM micrographs of SnO_2 films that were deposited on oxidized silicon substrate from various concentrations of H_2SiF_6. Based on previous experimental results, the films were calcined at 600 ˚C for 1 hour in air [22]. It is note that the as-deposited SnO_2 film prepared by LPD contain fluorine element that could be removed completely when the calcination

temperature was arrived at 600 °C and formed a pure SnO_2 film. The surface morphology and porosity of SnO_2 films were clearly varied with the Si/Sn molar ratio as shown in Fig. 4. The parameters of fabrication of the SnO_2 film were set as above, and a uniform and dense SnO_2 film was formed on the substrate surface without adding H_2SiF_6, as shown in Fig. 4(a). On the other hand, when the H_2SiF_6 solution was added into the growth solution, the Si species that were derived from the H_2SiF_6 solution agglomerated with Sn species and formed a porous SnO_2 film during the liquid phase deposition. The SiO_2-doped SnO_2 film was constructed of non-uniform particles with different sizes as shown in Fig. 4(b). This result suggests that the SiO_2-doped SnO_2 film is suitable for fabricating gas sensors because it is porous with a large surface area [10, 23].

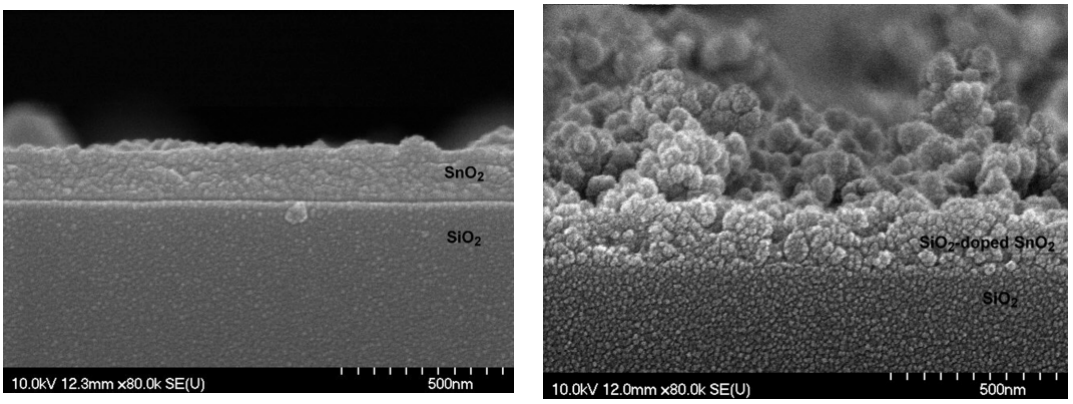

(a) (b)

Fig. 4. SEM micrographs of SnO_2 films deposited from various concentrations of H_2SiF_6 after calcination at 600 °C for 1 hour in air. (a) pure SnO_2 and (b) Si/Sn (0.5).

Figure 5 shows the AFM photographs of SnO_2 films deposited from various concentrations of H_2SiF_6 and calcined at 600 °C for 1 hour in air. The surface morphology of pure SnO_2 film revealed a uniform particle size and high surface coverage (mean pore size is 43 nm), as shown in Fig. 5(a). For SiO_2-doped SnO_2 film, the particle size of the doped film exhibited non-uniformly distribution on the substrate surface. At Si/Sn molar ratio of 0.5, the porous structure was formed obviously by the particles (150~250 nm in size) contacted each other to form a large pores (126 nm average in size), and the grain size of SnO_2 was kept about 5 nm. This result shows that the introduction of SiO_2 tended to inhibit the grain growth of SnO_2 and enhanced the porosity of SnO_2 film. Furthermore, the surface roughness of the film

increased with the concentration of H_2SiF_6 solution, as shown in Figs. 5(b), consistent with the SEM results shown in Fig. 4(b).

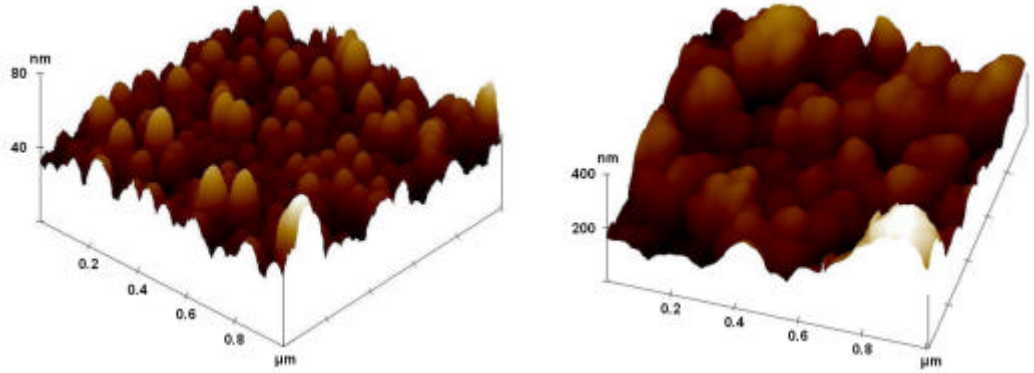

(a) (b)

Fig. 5. AFM photographs of SnO_2 films deposited from various concentrations of H_2SiF_6 after calcination at 600 °C for 1 hour in air. (a) pure SnO_2 and (b) Si/Sn (0.5).

3.2 Stoichiometric analysis of thin films

The surface compositions of the SiO_2-doped SnO_2 films were analyzed by high resolution X-ray photoelectron spectroscopy (HRXPS). To generate atomic percentage values, each raw XPS signal must be corrected by dividing its signal intensity (number of electrons detected) by a relative sensitivity factor (RSF) and normalized over all of the elements detected [24], as given in Table 1. The analysis reveals that the atomic concentration of Si was very small (1%~2.5%) in the SnO_2 films that were deposited from Si/Sn molar ratio at 0.25~0.33. However, when the molar ratio was increased to 0.5, the atomic concentration of Si increased considerably to 6.75 %.

Table 1. Surface compositions of the deposited films

LPD SnO_2 thin film	Atomic concentration				
	Sn (%)	Si (%)	O (%)	Al (%)	Total (%)
Pure SnO_2	31.54	0	68.46	0	100
Si/Sn(0.25)	31.26	1.36	67.38	0	100
Si/Sn(0.33)	29.03	2.44	68.53	0	100
Si/Sn(0.5)	25.38	6.75	67.87	0	100

Figure 6 shows the results of the depth profile analysis (after correction for the atomic sensitivity factors) of the SnO_2 films prepared from H_2SiF_6 solution at various concentrations as a function of the sputtering time. It reports the O,

Sn, Si and Al elemental concentration in the films. For measurement purposes, since the amount of elemental Si in the doped films was very small, alumina was used as a substrate in place of the silicon wafer to prevent the HRXPS analysis results from being influenced by the Si substrate background signal. In Figs. 6, we observed that before the sputtering, the investigated LPD SnO_2 film consists of two dominant contributions: Sn and O corresponding to the pure SnO_2. When the SiO_2 introduced in the SnO_2 film, the film consists of three dominant contributions: Sn, Si and O corresponding to the mixture SnO_2 and SiO_2 as given in Table 1. The depth profile of the SnO_2 film (without SiO_2) clearly reveals that the atomic concentration of the Si did not change by increasing sputtering time, as shown in Fig. 6(a). In Figs. 6(b)–(c), the depth profiles of SiO_2-doped SnO_2 films prepared from Si/Sn molar ratios of 0.25 and 0.33 show that the amplitude of Si signal was increased slightly and contained only a small amount (1%–3%) in the SnO_2 film. This result indicated that the Si elements were uniformity dispersed in SnO_2 film. On the other hand, the atomic concentration of the Si changed considerably (about ~ 15 %) when the molar ratio reached 0.5, as shown in Fig. 6(d). These results show that various concentration of the Si atomic in the SnO_2 film could be obtained by controlling the Si/Sn molar ratio which confirmed that the Sn and Si elements were simultaneously present throughout the SnO_2 film during deposition.

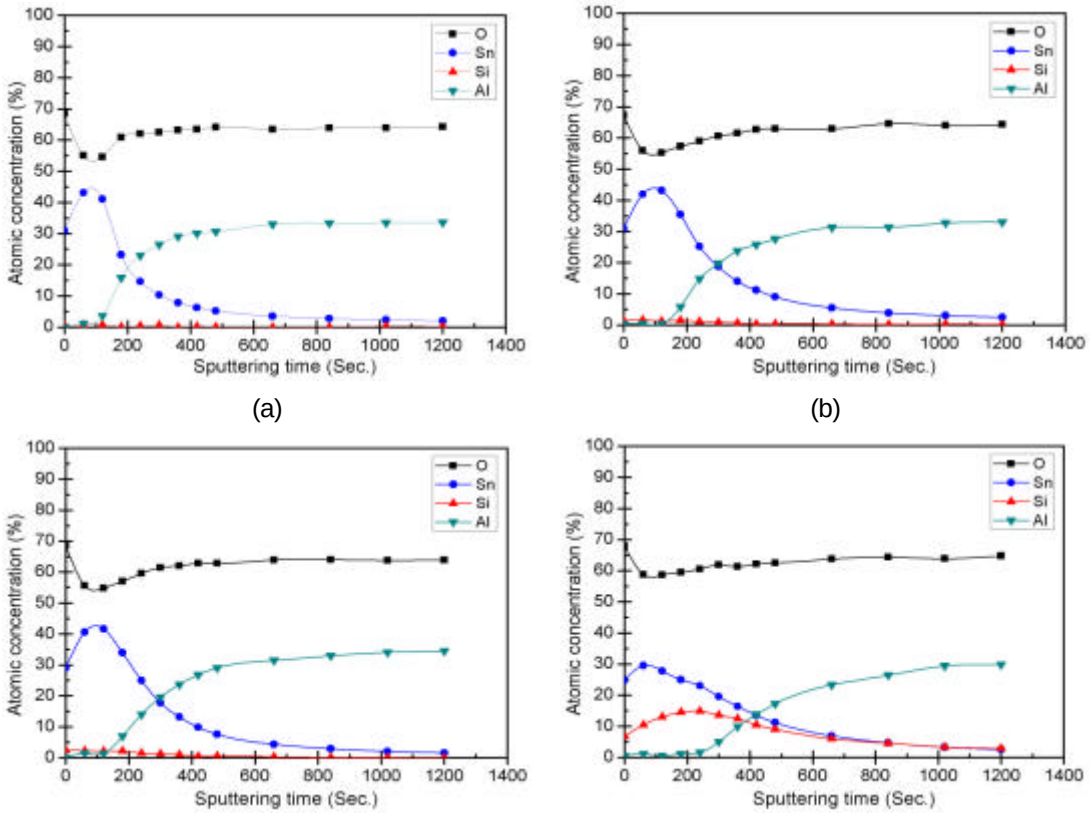

(a) (b)

(c) (d)

Fig. 6. Atomic concentration of O, Sn, Si and Al in sensing film as a function of the sputtering time: (a) pure SnO_2, (b) Si/Sn (0.25), (c) Si/Sn (0.33) and (d) Si/Sn (0.5).

3.3 Response characteristics of gas sensors to H_2S

Figure 7 shows the effect of SiO_2 additive on the gas concentration characteristics of the SnO_2 gas sensor with catalysts Au and Cu. The response plots of the gas sensors operated at the temperature of 270 °C as a function of concentration of H_2S gas are straight lines on logarithmic scales. In this study, the sensors have wide spreads of absolute values of resistance during the sensing process, for it effectively normalizes the parameter, which can clearly show that the resistance changed with increasing gas concentration at various Si/Sn molar ratios. According to Fig. 7, the relationship between the resistance ratio (R_s/R_o) of the sensor (where R_o is the sensor resistance in 1 ppm H_2S and R_s is the sensor resistance in various H_2S concentration) and the gas concentration can be expressed by the following equation over a certain range of gas concentrations [20].

$$R_r = A \times C_s^{\ a} \qquad (2)$$

where R_r denotes the resistance ratio (R_s/R_o) of the sensor, and C_s, A, and a denote gas concentration, a constant and the slope of the curve, respectively.

As shown in Fig. 7, since the differences in the resistance ratio R_r of each sensor responds to staircase concentration of H_2S gas were limited. By multiplying the multiple of 1 to 4 for sensors A to D, respectively, we can show the relationship between the R_r value and concentration of H_2S clearly. The result indicates that the value of α increased with the SiO_2 content derived from the H_2SiF_6 solution, suggesting that the SiO_2 additive affected the dependence of resistance on the gas concentration.

Figure 8 shows the sensitivity of sensors A to E, operated at 270 °C, to 2ppm H_2S gas. Experimental results indicated that the sensitivities of the sensors with catalysts Au and Cu were effectively enhanced by increasing the concentration of the SiO_2 additive. From this result, we concluded that the sensitivity of the sensors was increased due to the following two factors: (i) the target gas reacted with the catalyst, and (ii) the effective surface area of the sensor was exposed to ambiance of the target gas. The first factor was reported in a previous study [22], demonstrating that the catalysts Au and Cu

effectively enhance the sensitivity of sensors to H_2S gas. In this study, the CuO catalyst is used as a p-type semiconductor, which formed p-n junctions with the n-type SnO_2. The presence of these junctions leads to a higher resistive state of the sensor in air. When the sensor with CuO catalyst exposed to H_2S, CuO is converted to CuS. As CuS is an electronic conductance, which forming result in the destruction of p-n junctions and the resistance drops. When H_2S is turned off, CuS is quickly oxidized to CuO. The redox mechanism of the CuO catalyst is based on the reaction equation given as follows: [10, 25]:

$$CuO + H2S \rightarrow CuS + H2O \quad (3)$$

$$CuS + 3/2O_2 \rightarrow CuO + SO_2 \quad (4)$$

On the other hand, upon introducing Au catalyst to SnO_2 film, we are able to improve the drift response properties of gas sensor at long-term operation. As reported by Nelli et al. [26], cluster size and distribution of Au atoms in Au-doped SnO_2 film were not changed apparently after aging, which can be effectively limited the resistance drift of sensor during the long-term operation and consequently enhanced the long-term stability of sensor. In addition, according to Chiou et al. [22], an Au-doped SnO_2 film can also increase the sensitivity to H_2S gas. The increased sensitivity can be attributed to the partial oxidation of H_2S gas on the Au active metal and subsequent spillover of hydrogen atoms to the surface of SnO_2 substrate.

For the second factor, since the presence of the SiO_2 additive in a sensing film inhibited grain growth and effectively improved the surface areas of sensors B, C and D, agreeing with the XRD and SEM results herein. This result reveals that the sensors B to D have largest sensitivity than both sensor A and E at the concentration of 2ppm H_2S as shown in Fig. 8.

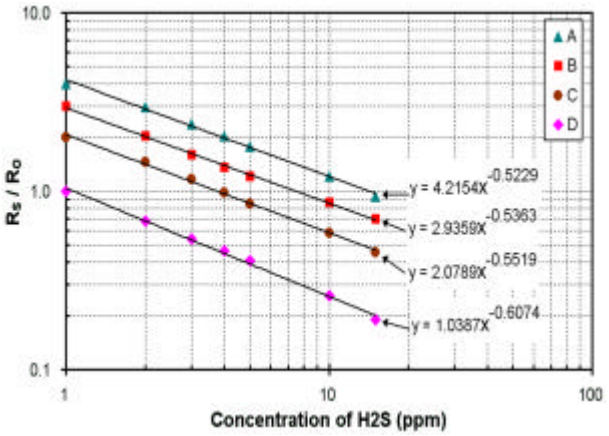

Fig. 7. Influence of SiO_2 additive on the gas concentration characteristics of the SnO_2-based gas sensors operated at 270 °C: (A) (Au, Cu)-doped SnO_2 film,

(B) (Au, Cu)-doped Si/Sn (0.25) film, (C) (Au, Cu)-doped Si/Sn (0.33) film and (D) (Au, Cu)-doped Si/Sn (0.5) film. *Ro*: sensor resistance in 1 ppm H_2S; *Rs*: sensor resistance in various H_2S concentration.

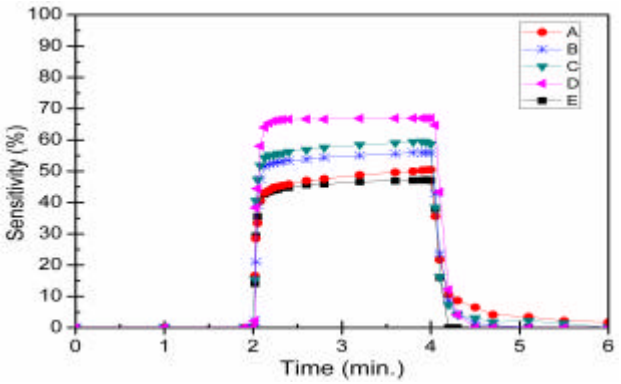

Fig. 8. The sensitivity to 2 ppm H_2S of sensors: (A) (Au, Cu)-doped SnO_2 film, (B) (Au, Cu)-doped Si/Sn (0.25) film, (C) (Au, Cu)-doped Si/Sn (0.33) film, (D) (Au, Cu)-doped Si/Sn (0.5) film and (E) pure SnO_2 film at 270 ºC.

The microstructure of a sensing film, including grain size, affects its sensing response and electrical properties. In the present study, four sensors A, B, C and D were prepared from H_2SiF_6 solution at various concentrations and coated with Au and Cu catalyst, with grain sizes of 7.9, 8.4, 6.5 and 4.7 nm, respectively. For electrical properties of sensors, the changes in resistance of the sensors were greatly influenced by grain size. As the result shown in Fig. 9, which is denoted to sensor from A to D, it is found that the electric resistances of the sensors operated at 270 ºC in air were changed by the effect of grain size. In this work, the effect of grain size on resistance of these sensors can be attributed to the factors of the neck-control and the grain-control [27]. For the sensors A to C, firstly, grain sizes of the sensors are larger than 2*L* (ca. 6nm) where *L* is the Debye length of SnO_2. The SnO_2 grains in the sensor are connected each other and formed a neck mold (belong to the neck-control). In the case, conduction electrons move through a channel penetrating each neck, so that the neck size in each SnO_2 grain is dominated mainly the resistance of the sensor. Under this condition, a decline in grain size would lead to slightly higher resistance of a sensor. Therefore, the resistance of sensors A to C would be located at the same magnitude of order in clear air. On the other hand, the grain size of the sensor D is smaller than 2*L*. Because whole grains are now put inside the space charge region, which lead to the grain boundary potential was maintained at high potential barrier level in ambient air. Hence, the resistance of the sensor was governed by the resistance of grains (belong

to the grain-control). Otherwise, due to the amount of insulating SiO_2 additive in the sensor D is largest compared with sensor A to C and thus the resistance of sensor D was drastically increased. By comparing the resistance of these sensors in ambient air, it can be seen that the resistance magnitude of sensor D is two orders larger than sensor A to C as shown in Fig. 9.

Figure 9 plots their electrical responses to ambient air and 5 ppm H_2S gas at operating temperature of 270 ºC. The results indicate that all of the sensors have highly reproducible and stable sensing characteristics during multiple cycles of sensing and recovery. Moreover, their electrical response is fast and highly reversible, during both sensing and recovery, and depends strongly on the grain size. Table 2 summarizes the 90 % times ($t_{90\%}$) for the response and recovery of sensors A to D. It reveals that the sensors respond very rapidly and their $t_{90\%}$ values were decreased by reducing the grain size. The results indicate that the grain size of the SnO_2 thin film affects the sensitivity and the response time.

Table 2. The response and recovery time of the SnO_2 sensors at operating temperature of 270 ºC for the detection of 5 ppm H_2S.

Sample Number	**Response time ($t_{90\%}$:s)**	**Recovery time ($t_{90\%}$:s)**
Sensor A	31	101
Sensor B	19	19
Sensor C	4	13
Sensor D	<3	12

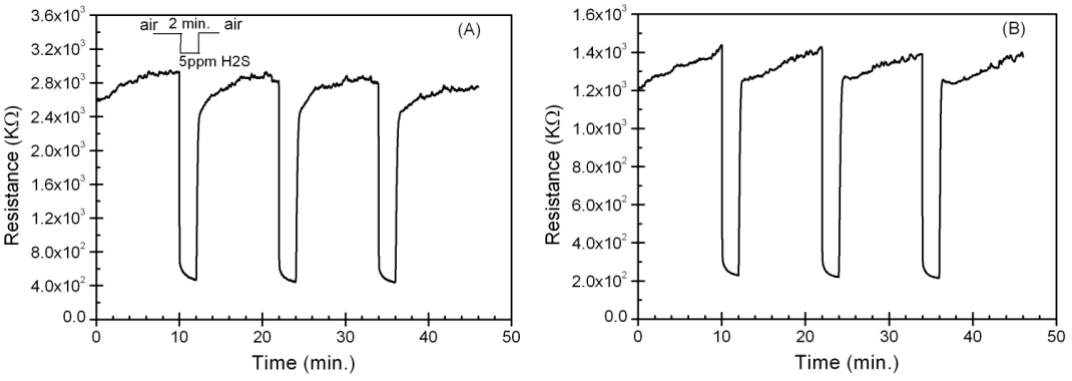

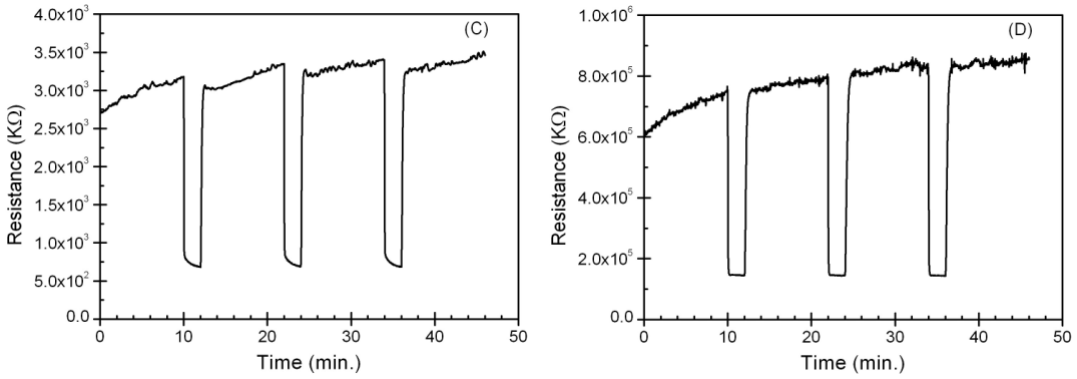

Fig. 9. The characteristics of response and recovery of sensors: (A) (Au, Cu) doped pure SnO_2, (B) (Au, Cu) doped Si/Sn (0.25), (C) (Au, Cu) doped Si/Sn (0.33) and (D) (Au, Cu) doped Si/Sn (0.5) to 5 ppm H_2S at 270 ºC.

4. Conclusion

In this study, a fabrication method that is based on liquid phase deposition was proposed firstly to fabricate a nano-crystalline SnO_2 sensing film. From characterization investigation of the sensor material, it is can be seen that the morphology of SnO_2 film changes significantly by increasing the concentration of H_2SiF_6 solution which decreases the grain size of SnO_2. The final stoichiometric analysis of the sensing material indicated that various concentration of the Si element in the SnO_2 film can be obtained by controlling Si/Sn molar ratio. For the sensing performance of H_2S gas, the SiO_2-doped Cu-Au-SnO_2 sensor presents better sensitivity compared to Cu-Au-SnO_2 sensor due to the fact that the distribution of SiO_2 particles in grain boundaries of nano-crystallines SnO_2 inhibited the grain growth (< 6 nm) and formed a porous film. Experimental results indicated that the SiO_2-doped Cu-Au-SnO_2 gas sensors (Si/Sn = 0.5) exhibit a good sensitivity (S = 67 %) to 2 ppm H_2S, a short response time ($t_{90\%}$ < 3 s) and a good gas concentration characteristic (α = 0.6074). Finally, the improvement of the nano-crystalline structures and high sensitivity for sensing films can be achieved by introducing SiO_2 additive into the SnO_2 film prepared by LPD method.

Acknowledgements

The authors would like to thank Dr. C.T. Huang from Oriental System Technology, Inc., Hsinchu Science Park, Taiwan for suggestions in gas sensor designs and fabrications. This work was supported in part by the Raydium Semiconductor Corporation, Taiwan, R. O. C. (contract no. 098426N3),

Ministry of Education (contract no. 99W958) and Taiwan Department of Health Clinical Trial and Research Center of Excellence (contract no. DOH99-TD-B-111-004)

References

[1] T. F. Stoica, V. S. Teodorescu, M. G. Blanchin, T. A. Stoica, M. Gartner, M. Losurdo, M. Zaharescu, Morphology, structure and optical properties of sol-gel ITO thin films, Mater. Sci. Eng. B 101 (2003) 222-226.

[2] T. Stergiopoulos, I. M. Arabatzis, H. Cachet, P. Falaras, Photoelectrochemistry at SnO2 particulate fractal electrodes sensitized by a ruthenium complex Solid-state solar cell assembling by incorporating a composite polymer electrolyte, J. Photochem. Photobiol. A 155 (2003) 163-170.

[3] Z. Tianshu, P. Hing, Y. Li, Z. Jiancheng, Selective detection of ethanol vapor and hydrogen using Cd-doped SnO_2-based sensors, Sens. Actuators B 60 (1999) 208-215.

[4] P. G. Harrison, C. Bailey, W. Azelee, Modified Tin (IV) Oxide (M/SnO2 M=Cr, La, Pr, Nd, Sm, Gd) catalysts for the Oxidation of Carbon Monoxide and propane, J. Catal. 186 (1999) 147-159.

[5] J. Tamaki, K. Shimanoe, Y. Yamada, Y. Yamanoto, N. Miura and N. Yamazoe, Dilute hydrogen sulfide sensing properties of CuO-SnO_2 thin film prepared by low-pressure evaporation method, Sens. Actuators B 49 (1998) 121-125.

[6] Z. Jin, H. J. Zhou, Z. L. Jin, R. F. Savinell, C. C. Liu, Application of nano-crystalline porous tin oxide thin film for CO sensing, Sens. Actuators B 52 (1998) 188–194.

[7] T. R. Ling, C. M. Tsai, Influence of nano-scale dopants of Pt, CaO and SiO2, on the alcohol sensing of SnO2 thin films, Sens. Actuators B 119 (2006) 497-503.

[8] J. Gong, Q. Chen, M. –R. Lian and N. –C. Liu, Micromachined nanocrystalline silver doped SnO2 H2S sensor, Sens. Actuators B 114 (2006) 32-39.

[9] C. Jin, T. Yamazaki, K. Ito, T. Kikuta, N. Nakatani, H_2S sensing property of porous SnO_2 sputtered films coated with various doping films, Vacuum 80 (2006) 723-725.

[10] G. Mangamma, V. Jayaraman, T. Gnanasekaran, G. Periaswami, Effects of silica additions on H2S sensing properties of CuO-SnO2 sensors, Sens. Actuators B 53 (1998) 133-139.

[11] N. Yamazoe, Y. Kurokawa and T. Seiyama, Effects of additives on semiconductor gas sensors, Sens. Actuators 4 (1983) 283-289.

[12] C. Xu, J. Tamaki, N. Miura and N. Yamazoe, Grain size effects on gas sensitivity of porous SnO_2-based elements, Sens. Actuators B 3 (1991) 147-155.

[13] N. L. Wu, S. Y. Wang, I. A. Rusakova, Inhibition of Crystallite Growth in the Sol-Gel Synthesis of Nanocrystalline Metal Oxides, Science 285 (1999) 1375-1377.

[14] S. Rani, S. C. Roy, M. C. Bhatnagar, Effect of Fe doping on the gas sensing properties of nano-crystalline SnO2 thin films, Sens. Actuators B 122 (2007) 204-210.
[15] J. Zhu, B. Y. Tay, J. Ma, Hydrothermal synthesis and characterization of mesoporous SnO2/SnO2-SiO2 on neutral template, J. Mater. Process. Technol. 192-193 (2007) 561-566.
[16] D. D. Vuong, G. Sakai, K. Shimanoe, N. Yamazoe, Preparation of grain size-controlled tin oxide sols by hydrothermal treatment for thin film sensor application, Sens. Actuators B 103 (2004) 386-391.
[17] K. Tsukuma, T. Akiyama, H. Imai, Liquid phase deposition film of tin oxide, J. Non-Cryst. Solids 210 (1997) 48-54.
[18] S. Deki, Y. Aoi, O. Hiroi and A. Kajinami, Titanium (IV) Oxide Thin Films Prepared from Aqueous Solution, Chem Lett. (1996) 433-434.
[19] M. Izaki, T. Omi, Transparent Zinc Oxide Films Chemically Prepared from Aqueous Solution, J. Electrochem. Soc., 144 (1997) L3-L5.
[20] K. Ihokura, J. Watson," The stannic oxide gas sensor: principles and applications", Boca Raton, CRC Press, 1994.
[21] A. L. Patterson, The Scherrer Formula for X-Ray Particle Size Determination, Phys. Rev. 56 (1939) 978–982.
[22] J. C. Chiou, S. W. Tsai, Y. S. Liu and C. T. Huang, Effect of Depositing Tin Oxide Thin Film in Liquid Phase Deposition and Dip-Coating Cu and Au Catalysis on H2S Gas-Sensing Performance, Sens. Mater. 20 (2008) 425-433.
[23] N. Sergent, P. Gelin, L. Perier-Camby, H. Praliaud, G. Thomas, Preparation and characterisation of high surface area stannic oxides: structural, textural and semiconducting properties, Sens. Actuators B 84 (2002) 176-188.
[24] C. D. Wagner, L. E. Davis, M. V. Zeller, J. A. Tavlor, R. H. Raymond and L. H. Gale, Empirical atomic sensitivity factors for quantitative analysis by electron spectroscopy for chemical analysis, Surf. Interface Anal. 3 (1981) 211-225.
[25] T. Maekawa, J. Tamaki, N. Miura and N. Yamazoe, Improvement of Copper Oxide-Tin Oxide Sensor for Dilute Hydrogen Sulfide, J. Mater. Chem. 4 (1994) 1259-1262.
[26] P. Nelli, G. Faglia, G. Sberveglieri, E. Cereda, G. Gabetta, A. Dieguez, A. R.-Rodriguez and J. R. Morante, The aging effect on SnO_2- Au thin film sensors: electrical and structural characterization, Thin Solid Films 371 (2000) 249-253.
[27] C. Xu, J. Tamaki, N. Miura and N. Yamazoe, Grain size effects on gas sensitivity of porous SnO_2- based elements, Sens. Actuators B 3 (1991) 147-155.

Biographies

Jin-Chern Chiou received MS and PhD degrees in aerospace engineering science from the University of Colorado at Boulder in 1986 and 1990, respectively. His research interests include microelectromechanical systems (MEMS), biosensors, servo control, and modeling and control of multibody dynamic systems (MBDs). Currently, Dr. Chiou is a professor in the Department of Electrical Engineering, National Chiao Tung University, director of the Biomedical Engineering Research and Development Center of China Medical University.

Shang-Wei Tsai received MS degree in mechanical and computer-aided engineering from Feng Chia University at Taichung, Taiwan (R.O.C.) in 2004. His is now a PhD student at Institute of Electrical and Control Engineering under the supervisor of prof. J. C. Chiou. His main research fields include gas sensing performance of metal oxide semiconductor thin films, microsystem design and fabrication.